ACTA ODONTOLOGICA SCANDINAVICA, 2016
VOL. 74, NO. 7, 539–549
http://dx.doi.org/10.1080/00016357.2016.1214980

Taylor & Francis
Taylor & Francis Group

ORIGINAL ARTICLE

LS8 cell apoptosis induced by NaF through p-ERK and p-JNK – a mechanism study of dental fluorosis

Lin Zhao[a,b], Juedan Li[a], Jiali Su[a,d], Malcolm L. Snead[c] and Jianping Ruan[a]

[a]Clinical Research Center of Shaanxi Province for Dental and Maxillofacial Diseases, Department of Preventive Dentistry, Stomatology Hospital, Xi'an Jiaotong University, Xi'an, PR China; [b]Department of Oral Pathology, Stomatology Hospital, Ningxia Medical University, Yinchuan, PR China; [c]Herman Ostrow School of Dentistry of USC, Center for Craniofacial Molecular Biology, University of Southern California, Los Angeles, CA, USA; [d]Department of Endodontics, Yinchuan Stomatology Hospital, Yinchuan, PR China

ABSTRACT

Objective: To investigate the possible biological mechanism of dental fluorosis at a molecular level.

Material and methods: Cultured LS8 were incubated with serum-free medium containing selected concentrations of NaF (0 ~ 2 mM) for either 24 or 48 h. Subcellular microanatomy was characterized using TEM; meanwhile, selected biomolecules were analysed using various biochemistry techniques. Transient transfection was used to modulate a molecular pathway for apoptosis.

Results: Apoptosis of LS8 was induced by NaF treatment that showed both time and concentration dependency. The activity of caspase-3, -8, -9 was found to be increased with NaF in a dose-dependent manner. Western blot revealed that the protein expression of p-ERK and p-JNK were decreased, while the expression of p-P38 was increased. Inhibition of the p-ERK and p-JNK pathways resulted in a similar decrease for caspase-3.

Conclusion: During NaF-induced apoptosis of LS8, p-ERK and p-JNK were closely associated with induction of apoptosis, which might be a mechanism of dental fluorosis.

ARTICLE HISTORY
Received 25 March 2016
Revised 11 July 2016
Accepted 16 July 2016
Published online 12 September 2016

KEYWORDS
NaF; LS8; apoptosis; mitogen-activated protein kinase; dental fluorosis

Introduction

The beneficial role of fluoride for health through caries prevention is well-accepted.[1–3] A number of approaches have been used to deliver fluoride to the oral cavity, such as water fluoridation, toothpaste, mouthwash [4–6] and fluoride releasing restorative materials.[7] However, systemic fluoride administration must not exceed the recommended dosage since higher fluoride concentrations exert adverse effects. For example, excessive fluoride intake during tooth development has been linked to dental fluorosis, which in severe form leads to brownish discoloration of teeth, surface pitting and susceptibility for enamel destruction through caries.[8,9] An increased prevalence of this condition has been recently observed both in fluoridated and non-fluoridated areas.[5,10] However, other studies suggest fluoride opacities are not accompanied by lower caries prevalence.[10] Dental fluorosis is a clear oral manifestation of fluoride toxicity.[11,12] In addition, systemic delivery of excessive fluoride may produce diverse metabolic changes, such as alterations in membrane receptors, imbalances for energy metabolism, and DNA breaks, with the induction of apoptosis.[13–15]

Induction of apoptosis is among the most common and detrimental toxic effect of excessive fluoride on various types of cells, for example, lung epithelia cells,[16] renal epithelia cells,[17] osteoblasts,[18–20] odontoblasts [21–23] and gingival fibroblasts.[24] Similarly, the administration of sodium fluoride (NaF) has been linked to apoptotic cell death in ameloblast cells, including zebra fish inner enamel epithelium cells,[25] mouse ameloblast derived cells [26,27] and ameloblast-lineage cells isolated from the human enamel organ.[28] However, the exact signalling mechanisms causing ameloblast apoptosis due to fluorosis is not well understood.

Cellular mitochondrial components and pathways can play significant role in physiologic, as well pathologic conditions.[29] Mitogen-activated protein kinases (MAP kinases) include extracellular signal-regulated kinase (ERK), c-Jun N-terminal kinase (JNK) and p38.[30] Fluoride induced apoptosis of epithelial lung cells has been shown to occur through activating p38 and possibly the JNK pathway.[16] NaF induced apoptosis in odontoblast-like cells has been shown to be dependent on the JNK and ERK pathways.[21,23] However, there is very limited information on the effects of fluoride on MAPKs signalling pathway on ameloblast-like cells that can serve as a model to mimic the development of enamel during amelogenesis. The aim of this study was to investigate the roles of MAPK in fluoride-induced apoptosis of LS8 – an ameloblast-like cell line from mouse odontogenic epithelia. In addition, the possible biological mechanism of dental fluorosis was studied at the molecular level.

CONTACT Jianping Ruan ruanjp@mail.xjtu.edu.cn Department of Preventive Dentistry, Stomatology Hospital, Xi'an Jiaotong University, 98Xiwu Road, Xi'an 710004, Shaanxi, PR China

Materials and methods

Cell culture reagents and antibodies

Rabbit anti-phospho-p44/42 ERK (#9101), phospho-p38 (Thr180/Tyr182) (#9215), phospho-SAPK/JNK (Thr183/Tyr185) (#4671), anti-ERK (#9102), anti-P38 (#9212), anti-JNK (#9252), anti-caspase-3 (#9662), anti-caspase-8 (#4790), anti-caspase-9 (#9506) and anti-caspase-12 (#2202) were purchased from Cell Signalling (Beverly, MA). All antibodies were used at a dilution ratio of 1:500 ~1:1000 for western blot analysis. A β-actin antibody (#47778) was purchased from Santa Cruz Biotechnology (Santa Cruz, CA). Inhibitors (SB203580, SP600125 and PD98059) were purchased from Cell Signalling (Boston, MA). Curcumin was purchased from Sigma Aldrich Fluka (St. Louis., MO). Antisomycin was purchased from Melone Pharma (Melone Pharmaceutical Co., Ltd., Dalian, PR China). The inhibitors and activators were dissolved separately in dime thylsulfoxide (DMSO, Sigma, MO) immediately before use. Anti-rabbit and anti-mouse secondary antibody was purchased from Zhongshan Biological Manufacture (Zhongshan Co., Ltd, Beijing, PR China). Dulbecco's modified Eagle's medium (DMEM) was supplied by Thermo Scientific Company (Logan, UT). Fetal bovine serum (FBS) was supplied by Gibco (GIBCO, Invitrogen, CA), Lipofectamine 2000 Transfection Reagent was purchased from Invitrogen (Carlsbad, CA). Trizol Reagent was purchased from Invitrogen (Carlsbad, CA). Silencing RNAs (siRNAs) that specifically target mouse p38 and control siRNA, or FAM-labelled negative control siRNA were purchased from Gene Pharma (Gene Pharma Co., Ltd, Shanghai, PR China). All procedures were conducted with approval from the Ethics Committee at Xi'an Jiaotong University, Xi'an, PR China.

Cell culture and treatments

The mouse ameloblast-like cell line (LS8) was cultured in DMEM supplemented with 10% FBS and 100 units/mL penicillin, and 100 mg/mL streptomycin (Invitrogen, CA). The incubator atmosphere was humidified and adjusted at 5% CO_2 and 95% air at 37 °C. When the cells reached 70–80% confluence, they were incubated with serum-free medium containing the indicated concentrations (0 ~ 2 mM) of NaF. Cultured cells were incubated for either 24 or 48 h at 37 °C, as denoted in the text. Cells were collected and processed for further experiments.

Measurement of cell viability

LS8 cells were processed for determination of cell viability after fluoride exposure using the MTT [3-(4,5-dimethylthiazol-2-yl)-2,5-diphenyltetrazolium bromide] (Sigma, MO) dye method. Briefly, cells were plated at a density of 5,000 cells/well in 96-well plates. At a cell confluence value of circa 70%, culture medium was changed and cells were incubated for 48 h in100 μL medium containing varying doses of NaF (0, 0.5, 1.0,1.5, 2.0 mmol/L). Sodium chloride (NaCl) solution with the same concentrations (0, 0.5, 1.0, 1.5, 2.0 mmol/L) was used as control. A 20 μL aliquot of MTT dye was added to individual wells and absorbance was measured at 490 nm using a microplate reader (Bio-Rad model 680, Hercules, CA) to discriminate live versus dead cells and the data was digitally recorded.

Annexin V-FITC/propidium iodide staining

Annexin V-FITC/PI apoptosis detection kit (7Sea, Shanghai, PR China) was used to evaluate apoptosis according to the manufacturer's instructions. The LS8 (1×10^6 cells/well) were seeded in 6-well plates and cultured overnight. Following NaF treatment, the cells were released from the plate using brief trypsin digestion (2.5 mg/mL) and washed twice using chilled phosphate-buffered saline (PBS, pH 7.4) before suspending in binding buffer (provided by manufacturer). The cells were re-suspended in 400 μL of binding buffer and an aliquot of 5 μL of FITC-labelled annexin V was added. The cells were incubated at room temperature for 15 min. Thereafter, propidium iodide (PI) solution (10 μL) (provided by manufacturer) was added to the cells followed by an additional 5 min incubation. The ratio of live to apoptotic cells was detected using flow cytometry.

Electron microscopy

For electron microscopy, LS8 cells were treated with 2.0 mmol/L NaF for 48 h before imaging. As before, the harvested cells were recovered by brief trypsin digestion and centrifuged at 800 rpm for 10 min to collect the cells, which were fixed using 2.5% formaldehyde for 24 h at 4 °C. Subsequently, the samples were treated with 1% osmic acid for 1 h, dehydrated through a gradient ethanol series, embedded and ultrathin sections of silver refraction were prepared and placed on a TEM grid. The sections were stained with uranyl acetate and lead citrate and observed on a transmission electron microscope (JEM-ARM200F Hitachi, Tokyo, Japan). Representative images of the treated cells were captured digitally.

Measurement of caspase activity

Caspase activity was assessed using the caspase-8, -9, -3-assay kit (Beyotime Biotechnology, Shanghai, PR China) according to the manufacturer's instructions. Caspase activities were determined by a colorimetric assay based on the ability of caspase-8, -9, -3 to chemically transform substrates of acetyl-Ile-Glu-Thr-Asp p-nitroanilide (Ac-IETD-pNA), acetyl-Leu-Glu-His-Asp-nitroanilide (Ac-LEHD-pNA) and acetyl-Asp-Glu-Val-Aspp-nitroanilide (Ac-DEVD-pNA) into a yellow formazan product p-nitroaniline (pNA). Briefly, LS8 cells were treated using variable concentrations of NaF (0, 0.5, 1.0, 1.5, 2.0 mM) for 48 h, rinsed with ice-cold PBS pH 7.4, and disrupted with 40 μL of lysis buffer provided by manufacturer for 15 min on ice. Cell lysates were cleared by centrifugation at 20,000 × *g* for 15 min 4 °C and caspase-8, -9, -3 activity in the supernatant was assayed. Caspase transformed chromogenic substrate absorbance at 490 nm was used to quantify the caspase activity compared to control.

Preparation of cell fractions

LS8 cells were washed with chilled PBS and lysed in ice-cold RIPA buffer as previously described, consisting of 50 mM Tris–HCl, pH 7.5, 50 mM NaCl, 5 mM EDTA, 10 mM EGTA, 2 mM sodium pyrophosphate, 4 mM paranitrophenyl phosphate, 1 mM sodium orthovanadate, 1 mM phenylmethylsulfonyl fluoride, 2 μg/mL aprotinin, 2 μg/mL leupeptin and 2 μg/mL pepstatin.[31] Cell lysate was collected using a cells scraper (Corning, Acton, MA) and the homogenates sonicated on ice for 30 min. The lysate was collected by centrifugation at 12,000 $\times g$ for 15 min at 4 °C. The protein content was determined using a BCA protein assay kit (Pierce, Rockford, IL) by extrapolation to dye binding for a standard series of known protein concentration using spectrophotometry.

Western blotting

A volume of supernatant corresponding to an equal mass of protein for each experimental condition was mixed with loading buffer (5-sodium dodecyl sulphate, 5% v/v) and denatured by heating the samples at 95 °C for 5 min. Lysate proteins were resolved to size by electrophoresis using 10–12% sodium dodecyl sulphate polyacrylamide gel electrophoresis (SDS-PAGE) and transferred to 0.22 μm polyvinylidene fluoride (PVDF) membrane (Millipore, Bedford, MA) using a semi-dry blotting system (Bio-Rad, Hercules, CA). Non-specific absorption by the membranes was blocked by incubation with 5 g% (w/v) skin milk in Tris-buffered saline (TBS, 500 mM NaCl, 20 mM Tris–HCl pH 7.5, with 0.05% (v/v) Tween-20) for 2 h. Samples were incubated overnight with one of the following primary antibodies at 4 °C: anti-phospho-ERK (1:1000), anti-phospho-JNK (1:500), anti-phospho-p38 (1:500), anti-caspase-8, -9, -12, -3 (1:1000), total ERK, p38, JNK and β-actin (1:1000) each diluted in TBS with 5% (v/v) bovine serum containing 0.1% Tween-20 for 24 h at room temperature with gentle shaking. The membranes were washed using 0.1% Tween-20 TBS three times for 10 min each and incubated with horseradish peroxidase conjugated anti-rabbit or anti-mouse secondary antibody (1:10000), as appropriate for each primary antibody, for 1 h at room temperature. After washing in TBS-0.1% Tween-20 three times, an enhanced chemiluminescence kit (Millipore, MA) was used to detect immunoreactive protein bands. Blots were immune-detected with an anti-β-actin antibody (1:1000) to confirm equal mass of protein loaded among samples. The intensity for each immunoreactive protein band was quantified using a Quantity One densitometer (BioRad, Hercules, CA).

Transient transfection siRNA

At 40% confluence, LS8 cells were transfected with silencing RNA (siRNA) against p38, using lipofectamine 2000 transfection reagent according to the manufacturer's recommendation. Briefly, p38-siRNA was diluted in serum-free culture medium with the transfection reagent, mixed by vortexing and incubated for 20 min at room temperature to allow for formation of the transfection complex and added to the cells for 24 h. The effectiveness of gene silencing was monitored by measuring the p38 levels in relation to GAPDH, as analysed by qRT-PCR for mRNA expression levels and by western blot analysis for protein expression levels. Cells transfected with p38-siRNA, were exposed to NaF for 48 h. The expression level of caspase-8, -9, -12, -3 was determined using western blot analysis.

RNA extraction and reverse transcription polymerase chain reaction (RT-PCR)

The total RNA of the cells was extracted using Trizol reagent (Carlsbad, CA) according to the manufacturer's instructions. The quality and quantity of the isolated RNA was tested using a NanoDrop 2000/2000C spectrophotometer measuring absorbance at 260/280 nm. First-strand c-DNA synthesis was performed on 2 μg of total RNA using reverse transcription with Real Master Mix (Thermo Fisher Scientific, Logan, UT). Quantitative real-time PCR was performed in a 10 μL reaction mixture system using an Applied Bio systems 7500 Real-Time PCR System (Thermo Fisher, Waltham, MA) with an initial denaturation of 5 min at 95 °C, followed by 40 cycles of 95 °C for 5 s, 60 °C for 30 s and 72 °C for 30 s. Primers used in the amplification were designed and synthesized by Gene Pharma (Gene Pharma Inc., Shanghai, PR China). The sequences of the PCR primers were as follows: siRNA-P38, 5′ -GGGTC ATGCT CTATC AGAT- 3′; GAPDH F: 5' GCTGAG TATGT CGTGG AGT3'; R: 5' GTTCA CACCC ATCAC AAAC3', was used as the internal control. A melting curve analysis was performed on each amplicon to ensure amplification of a single PCR product. The relative expression levels were calculated using the comparative threshold cycle (△△CT) method.[32]

Statistical analysis

Data analyses were performed using Statistical Product and Service Solutions (SPSS) version 17.0 (SPSS Inc., Chicago, IL). All data are expressed as mean ± standard deviation (SD) with each experiment performed in triplicate. Differences among groups were tested by one-way ANOVA or two-way ANOVA and the T test was used for individual comparisons. A value of $p < 0.05$ was considered statistically significant.

Results

NaF induces LS8 cells apoptosis

A significant increase in the apoptosis of LS8 cells was observed after exposure to 0.5, 1.0, 1.5 and 2.0 mM NaF ($p < 0.05$) compared to control group. Apoptosis of LS8 cells increased in a linear dose-dependent manner with increasing F^-concentrations (Figure 1(A,C)). FITC-annexin V/PI staining experiment coupled to flow cytometry analysis revealed that 48 h exposure of cells to NaF (0.5, 1.0, 1.5 and 2.0 mM) produced a linear increase in apoptotic cells by 2.27, 3.00, 3.84, and 5.29-fold, respectively ($p < 0.01$). In addition, LS8 cell apoptosis increased in time-dependent manner (Figure 1(B,D)). Cells exposed to 2.0 mM NaF for 12, 24 or 48 h and

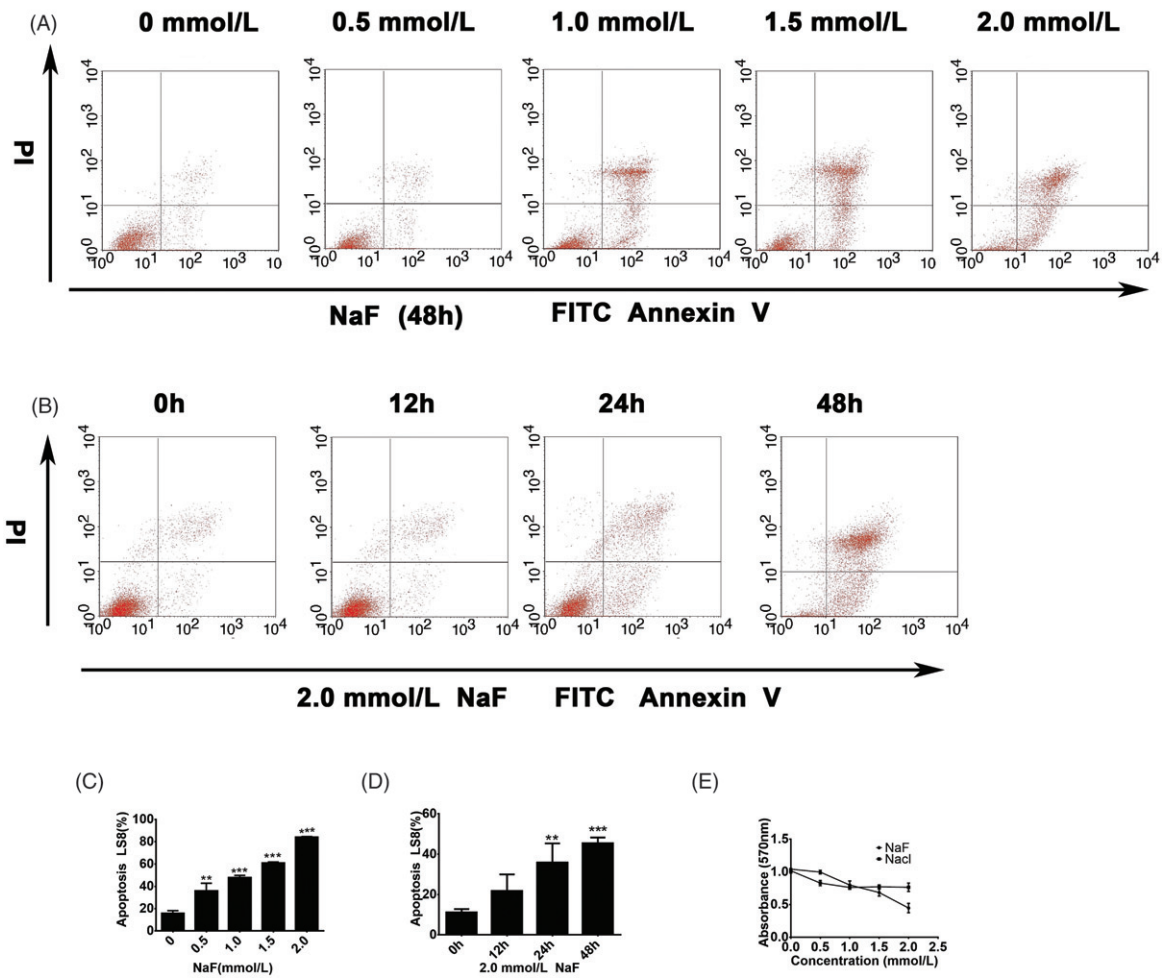

Figure 1. NaF treatment altered proliferation and induced apoptosis in LS8 ameloblast-like cells. LS8 cells (A, C) were incubated with 0, 0.5, 1.0, 1.5 and 2.0 mM NaF for 48 h (B, D) with 1.5 mM NaF for 0, 12, 24 and 48 h. Cell death was evaluated as described in methods and materials using flow cytometry detection of annexin-V with propidium iodine (PI) staining and interpreted as follows: Annexin V^-/PI^- viable cells; Annexin V^+/PI^-, early apoptotic cells; Annexin V^+/PI^+, late apoptotic cells; Annexin V^-/PI^+, necrotic cells. The results shown in panels A through D represent the mean ± standard of three independent experiments performed in triplicate, with the p value of <0.05 calculated using values from the control cells. Cell viability was determined by MTT exclusion assay after cells were incubated with 0, 0.5, 1.0, 1.5 and 2.0 mM NaF or NaCl for 48 h (E). The value shown in panel E is the mean ± SD of six samples, and represents percent survival relative to untreated control (0 mM NaF) cells.

examined by FITC-annexin V/PI staining revealed an increase in cell apoptosis by 1.95, 3.22, 4.08-fold, respectively ($p < 0.01$). Cell viability was examined using the MTT assay and after 48 h treatment with 0.5, 1.0, 1.5, 2.0 mM NaF, cell viability decreased to 11, 30, 40 and 61%, respectively ($p < 0.01$) (Figure 1(E)). LS8 cells exposed to 2.0 mM NaF for 48 h, revealed changes in their ultrastructure consisting of cell chromatin condensation, chromatin margination, nuclear fragmentation, membrane blebbing and the formation of apoptotic bodies (Figure 2).

Caspase activity in LS8 cells treated with NaF

In order to better define a potential candidate subcellular pathway associated with the above findings, we examined similarly treated cells by measuring their caspase-3 activity using DEVD-pNA as a substrate. The data revealed that NaF (1.5 and 2.0 mM) activated caspase-3 in LS8 cells with a measured activity of 65% ($p < 0.05$) and 73% ($p < 0.01$), respectively (Figure 3(E)). We used western immunoblot analysis to measure caspase protein in LS8 cells treated with 1.5 or 2.0 mM NaF concentration and found caspase-3 protein expression levels to be diminished when compared to control ($p < 0.05$) (Figure 3(A)). We also tested caspase-8 and -9-protein activity using Ac-IETD-pNA and Ac-LEHD-pNA peptides as substrate, respectively. NaF activated caspase-8 activity increased slightly with 1.5 or 2.0 mM NaF concentrations ($p < 0.05$) and caspase-9 activity increased with 2.0 mM NaF concentration ($p < 0.05$) (Figure 3(E)), whereas protein expression decreased ($p < 0.05$) (Figure 3(B,C)). In parallel experiments, caspase-12 protein expression was found to be decreased in cells treated with 1.5 and 2.0 mM NaF concentration ($p < 0.05$) (Figure 3(D)).

MAPK phosphorylation in LS8 cells treated with NaF

We treated LS8 with variable concentrations of NaF at different times as described in 'Materials and Methods' and explored changes to the phosphorylation of MAPK protein members by western immunoblot analysis. With exposure to NaF at 0.5, 1.0, 1.5 and 2.0 mM, the level of phosphorylated ERK (p-ERK) was decreased compared to the untreated

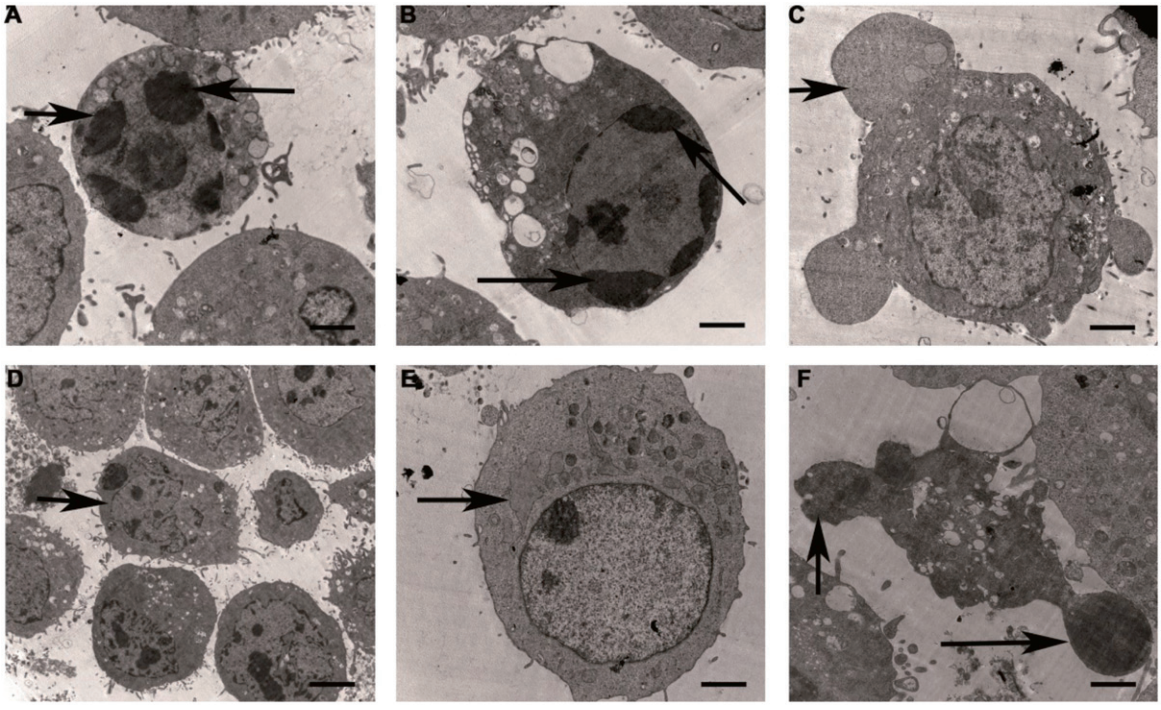

Figure 2. Transmission electron microscopy (TEM) images of the morphological features for LS8 ameloblast-like cells exposed to 2.0 mM NaF for 48 h. Typical features included: (A) cell chromatin condensation; (B) cell chromatin margination; (C) cell blebbing; (D, F) formation of apoptotic bodies with nuclear fragmentation and (E) endoplasmic reticulum expansion.
Scale bars, 2 μM.

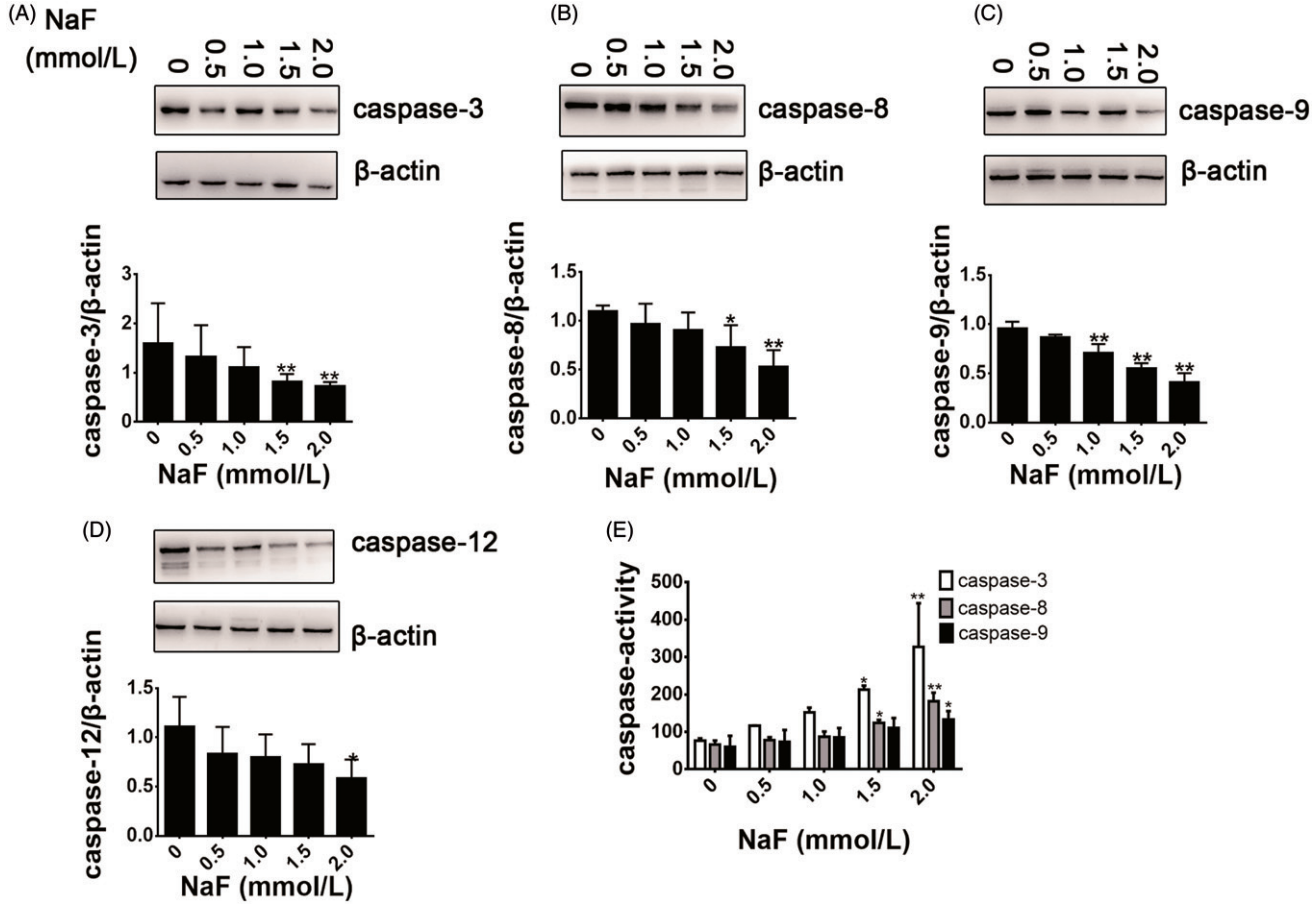

Figure 3. Expression levels and activity of selected caspase proteins in NaF-treated LS8 ameloblast-like cells. LS8 cells were treated for 48 h with either 0, 0.5, 1.0, 1.5 or 2.0 mM NaF, and expression of caspase-3, -8, -9 and -12 protein was detected using a caspase specific antibody by western blot analysis. The ratio of the caspase band intensity to the actin band intensity is graphed below each corresponding lane for: (A) caspase-3; (B) caspase-8; (C) caspase-9 and (D) caspase-12. For determination of caspase-3, -8 and -9 activity (E), the cells were treated with 0, 0.5, 1.0, 1.5 and 2.0 mM NaF for 48 h, and the cell lysates measured using a commercial caspase activity assay. The activity level of caspase-3, -8 and -9 was measured after treatment for 48 h with 0, 0.5, 1.0, 1.5 and 2.0 mM NaF. The data is represented as the mean ± SD. Statistical significance of: *, $p < 0.05$; **, $p < 0.01$ was by comparison with the untreated control.

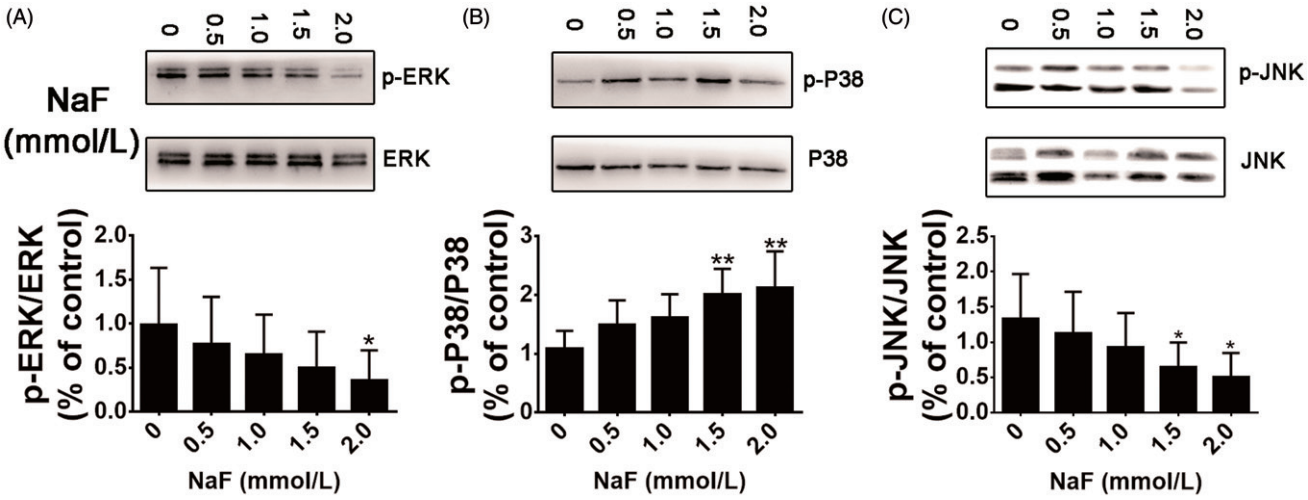

Figure 4. NaF-induced change in phosphorylation activation of signalling pathways in LS8 ameloblast-like cells. The phosphorylated- and non-phosphorylated-state of critical pathway elements include: (A) phosphorylated ERK (p-ERK); (B) phosphorylated p38 (p-P38) and (C) phosphorylated JNK (p-JNK). Cells were incubated 0, 0.5, 1.0, 1.5 and 2.0 mM NaF for 48 h, and cell lysates were subjected to western blotting with a specific antibody that discriminated the phosphorylated state from the native state. Each value (mean ± SD) is expressed as the ratio of the phosphorylated MAPK level to the corresponding total MAPK level. Statistically, *, $p < 0.05$, and **, $p < 0.01$ were determined by comparison to values from untreated control group (0 mM NaF).

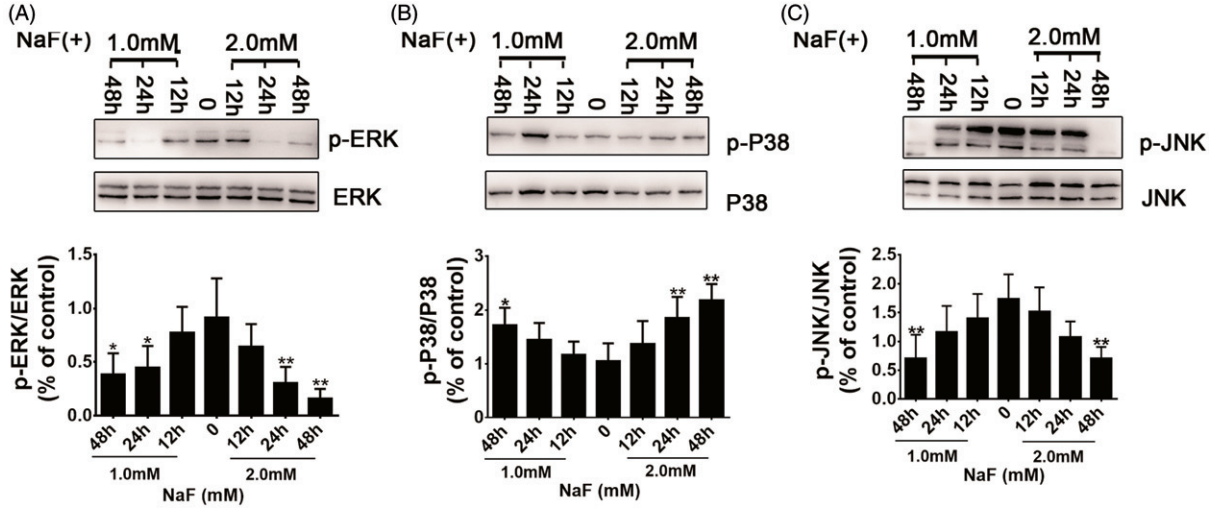

Figure 5. Time-course for NaF-induced quantitative change in the expression of p- ERK, p-p38 and p-JNK in LS8 ameloblast-like cells. Cells were incubated with 0, 1.0 and 2.0 mM NaF for 12, 24 and 48 h, and cell lysates were subjected to western blotting with antibodies specific for: (A) p-ERK, or total ERK; (B) p-p38, or total p38 and (C) p-JNK, or total JNK. Each value (mean ± SD) is expressed as the ratio of the phosphorylated MAPK level to the corresponding total MAPK level. Statistical significance for: *, $p < 0.05$; **, $p < 0.01$ was calculated versus values from the untreated control group (0 mM NaF).

group. Noteworthy, we observed that the level of p-ERK in cells treated by 2.0 mM NaF for 48 h decreased to 64% ($p < 0.05$) (Figure 4(A)). In LS8 cells treated with 1.5 and 2.0 mM NaF for 48 h, the level of phosphorylated p38 (p-p38) increased to 85 and 95% ($p < 0.01$), respectively (Figure 4(B)). Phosphorylated JNK (p-JNK) decreased to 52 and 62% ($p < 0.05$), respectively, in case of LS8 cells treated with 1.5 and 2.0 mM NaF for 48 h (Figure 4(C)). The data showed that p-ERK recovered from LS8 cells treated with 1.0 and 2.0 mM NaF at 24 or 48 h also decreased to 51, 58 ($p < 0.05$) and 67%, 83% ($p < 0.01$), respectively, when compared to control cell lysates (Figure 5(A)). The level of p-p38 detected in cells treated with 1.0 mM NaF for 48 h increased to 65% ($p < 0.05$), where as in contrast, cells treated with 2.0 mM NaF for 24 or 48 h revealed an increase in the amount of p-p38 to 77,108%, respectively ($p < 0.01$) (Figure 5(B)). Finally, cells treated with 1.0 or 2.0 mM NaF for 48 h revealed decreased p-JNK proteins expression to levels of 59 and 60%, respectively, compared to lysate from control cells ($p < 0.01$) (Figure 5(C)) while immunodetection for p-ERK and p-JNK decreased only modestly (Figure 6).

Western blot results for caspases

The western blot experiments revealed that when p-ERK or p-JNK was inhibited by PD98059 (Figure 7(A)) or SP600125 (Figure 7(C)), respectively, the expression of caspase-3 decreased, but the level of inhibition was not as great as that observed when cells were treated by NaF, even when both inhibitors and NaF were used. Caspase-3 protein levels were not changed significantly in LS8 cells treated by curcumin (Figure 7(B)) or anisomycin (Figure 7(D)). In addition, a lower degree reduction of caspase-3 was observed when LS8

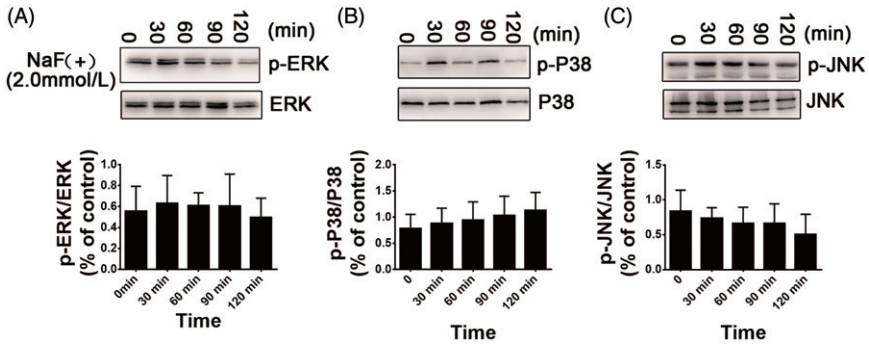

Figure 6. Time-course of NaF-induced changes of p-ERK, p-p38 and p-JNK in LS8 ameloblast-like cells. Cells were incubated in 1.5 mM NaF for 0, 30, 60, 90 and 120 min, and cell lysates were subjected to western blotting with an antibody that discriminates: (A) p-ERK, or total ERK; (B) p-p38, or total p38 and (C) p-JNK, or total JNK. Each value (mean ± SD) is expressed as the ratio of the phosphorylated MAPK protein level to the corresponding total MAPK protein level. No statistical significance was found when $p < 0.05$ was determined by calculation using values obtained from untreated control group (0 mM NaF).

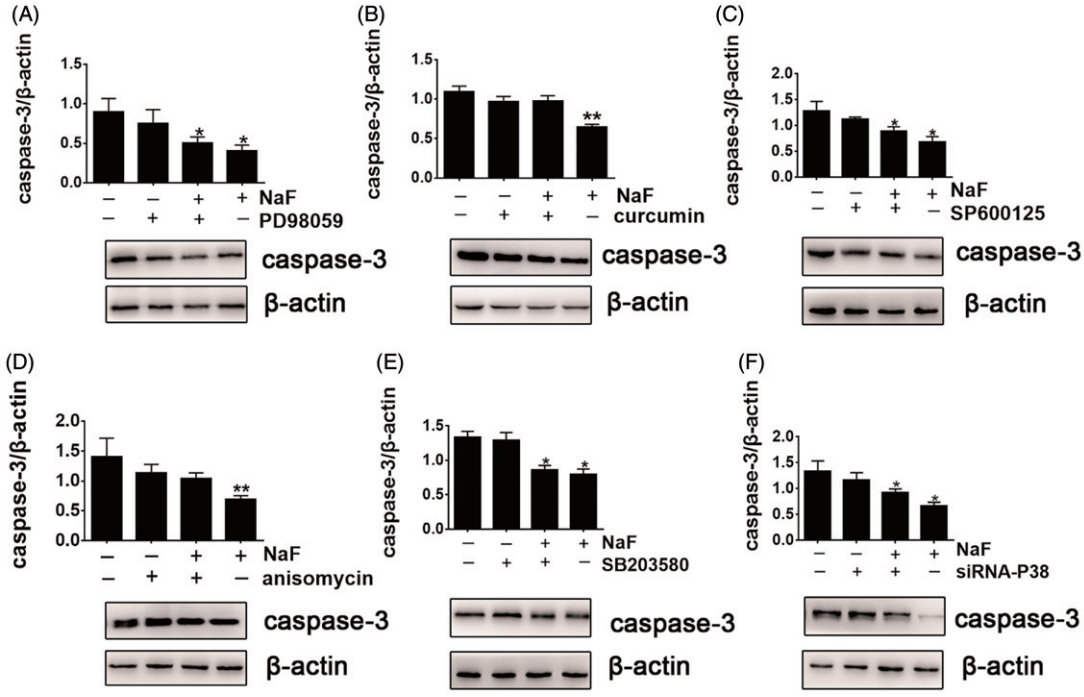

Figure 7. Effects of MAPK inhibitors, MAPK agonist and MAPK silencing RNA (siRNA) on NaF-induced caspase-3 expression in LS8 ameloblast-like cells. Cells were pre-incubated with (A) PD98059 (50 μM), or (B) curcumin (1 μM), or (C) SP600125 (50 μM), or (D) anisomycin (1 μM) or (E) SB203580 (20 μM) for 1 h, or with a MAPK siRNA followed by incubation with 1.5 mM NaF for 48 h. Cells lysates were subjected to western blot analysis with an antibody specific to caspase-3. Each value (mean ± SD) is expressed as a ratio of caspase-3 to β-actin protein level. Statistical significance of: *, $p < 0.05$; and **, $p < 0.01$ was determined by comparison to values from untreated control group.

cells treated by both NaF and agonist, either curcumin for ERK (Figure 7(B)) or anisomycin for JNK (Figure 7(C)), as compared with that of LS8 cells treated only by NaF. However, no expression changes of caspase-3 were observed when p38 was inhibited by SB203580 (Figure 7(E)) or siRNA-p38 (Figure 7(F)).

A similar pattern of accumulated protein expression for caspase-8 (Figure 8), caspase-9 (Figure 9) and caspase-12 (Figure 10) were observed when the LS8 cells were treated with either the inhibitors or agonists.

Discussion

Fluoride treatment has a profound beneficial effect on health by reducing mineral dissolution of fluoride substituted enamel hydroxyapatite, resulting in a reduction in dental caries and its comorbid diseases. Identifying fluoride susceptible pathways is a public health measure that may permit insights into the management for the potential adverse impact of excessive fluoride. In this study, we observed variation among ERK-, JNK-signalling molecules, as well as variation in endoplasmic reticulum dependent pathways involved in the NaF induced apoptosis of LS8-ameloblast like cells. Previous investigations have reported that the MAPK pathway was involved in tooth germ formation, supporting the notion that these pathways operate in the ameloblast cells that make the enamel bioceramic tissue.[33–35] Whereas, specific adverse cellular effects for fluoride treatment have been implicated, more research is needed to determine which of these changes are relevant to the development of dental

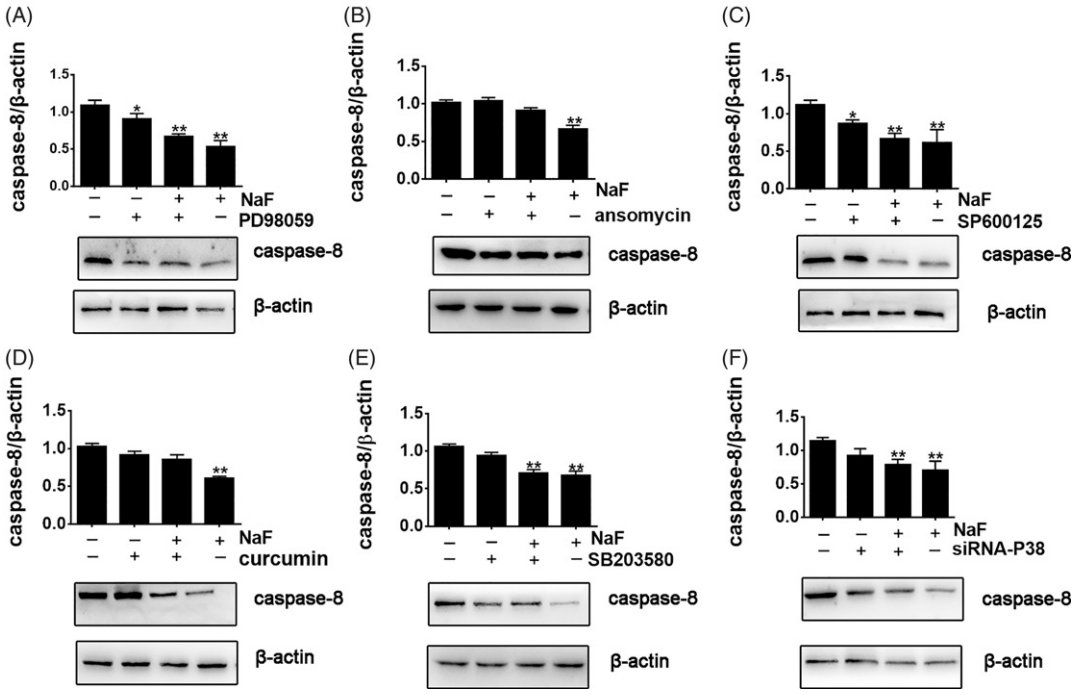

Figure 8. Effects of MAPK inhibitors, MAPK agonist and MAPK silencing RNA (siRNA) on NaF-induced caspase-8 expression levels in LS8 ameloblast-like cells. Cells were pre-incubated with either: (A) PD98059 (50 μM), or (B) anisomycin (1 μM); or (C) SP600125 (50 μM); or (D) curcumin (1 μM); or (E) SB203580 (20 μM) for 1 h; or with MAPK siRNA and incubated with 1.5 mM NaF for 48 h. Cells lysates were subjected to western blotting with an antibody specific for caspase-8. Each value (mean ± SD) is expressed as the ratio of caspase-8 to β-actin levels. Statistical significance of: *, $p < 0.05$; **, $p < 0.01$ was calculated based on values from untreated control group.

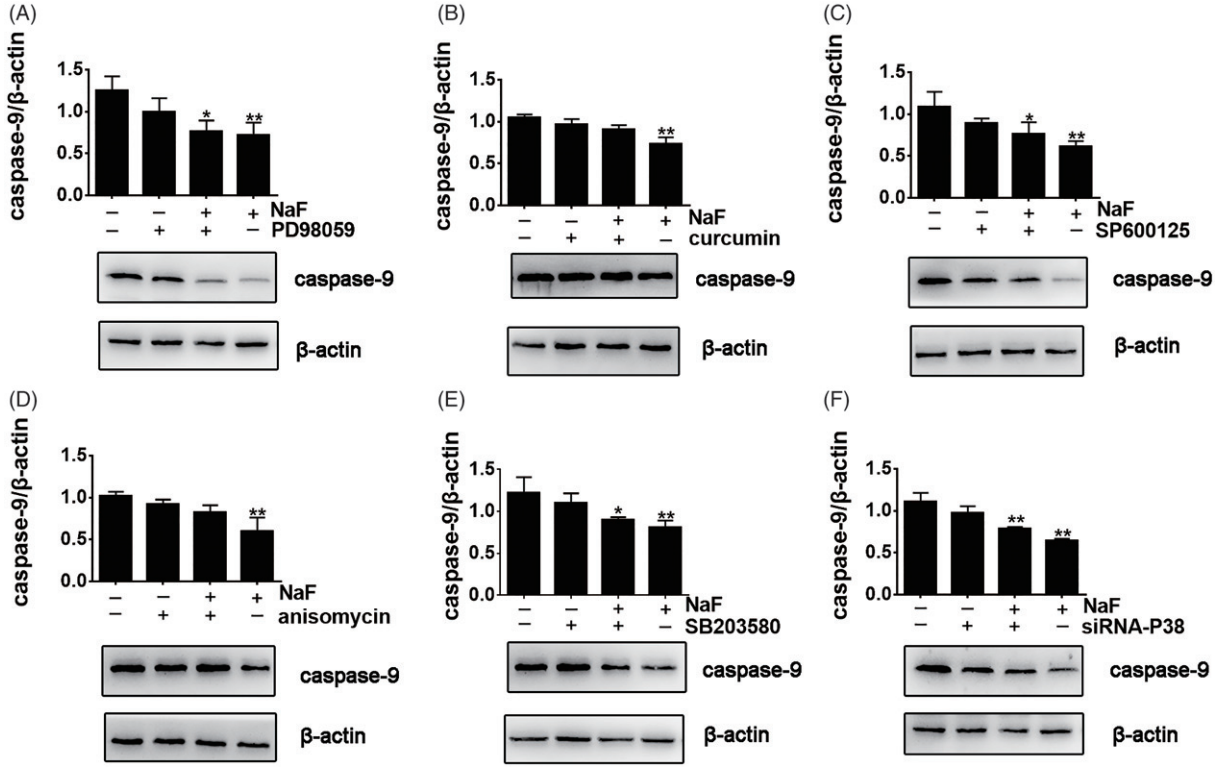

Figure 9. Effects of MAPK inhibitors, agonist and MAPK silencing RNA (siRNA) on NaF-induced caspase-9 expression in LS8 ameloblast-like cells. Cells were pre-incubated with (A) PD98059 (50 μM); or (B) curcumin (1 μM); or (C) SP600125 (50 μM); or (D) anisomycin (1 μM) or (E) SB203580 (20 μM) for 1 h followed by incubation with 1.5 mM NaF for 48 h; or LS8 cells were treated with MAPK siRNA (F) for 6 h and incubated with 1.5 mM NaF for 48 h. Cells lysates were subjected to western blot analysis with an antibody specific to caspase-9. Each value (mean ± SD) is expressed as the ratio of caspase-9 to β-actin. Statistical significance of: *, $p < 0.05$; **, $p < 0.01$ experimental value versus untreated control group.

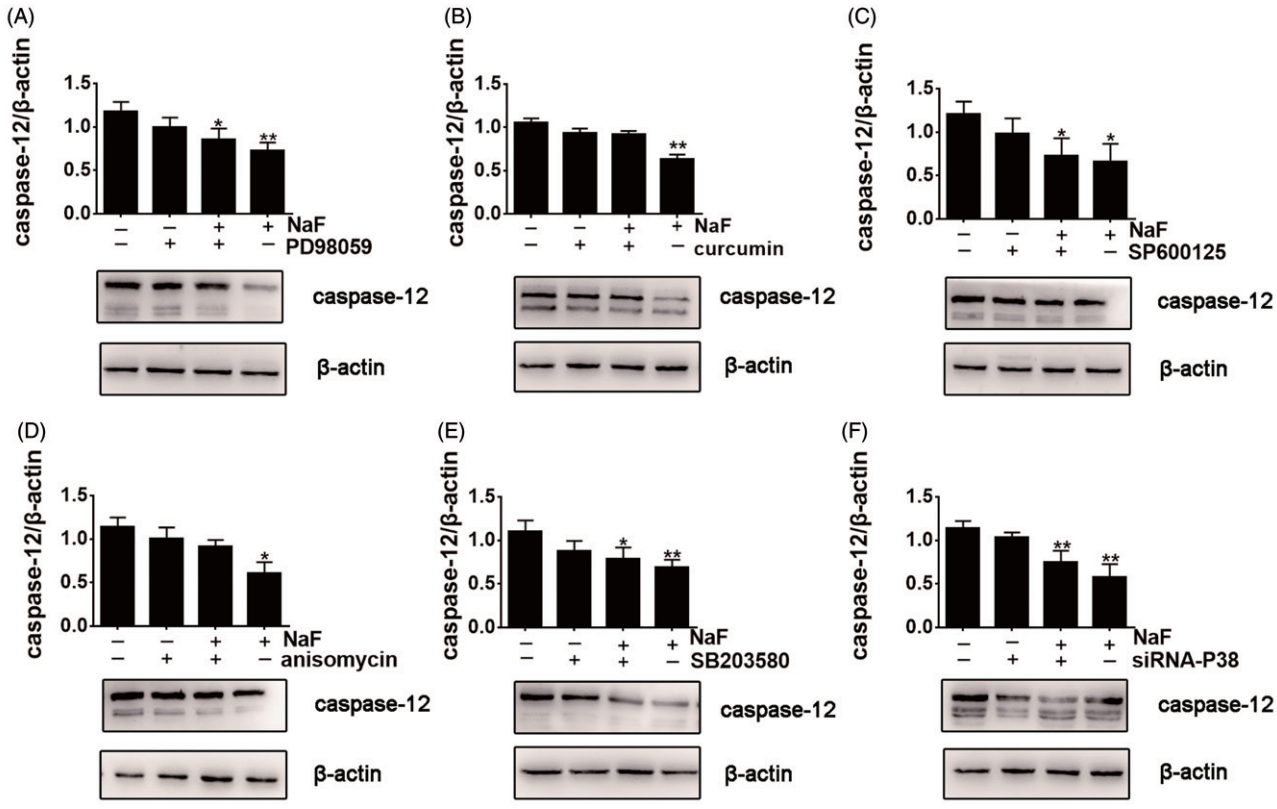

Figure 10. Effect of MAPK inhibitors, agonist and silencing RNA (siRNA) for MAPK on NaF-induced caspase-12 in LS8 ameloblast-like cells. Cells were pre-incubated with (A) PD98059 (50 μM); or (B) curcumin (1 μM); or (C) SP600125 (50 μM); or (D) anisomycin (1 μM) or (E) SB203580 (20 μM) for 1 h and incubated with 1.5 mM NaF for 48 h. Cells were treated with (F) MAPK siRNA for 6 h and incubated with 1.5 mM NaF for 48 h. Cells lysates were subjected to western blot analysis with detection by acaspase-12 specific antibody. Each value (mean ± SD) is expressed as the ratio of caspase-12 to β-actin. Statistical significance of: *, $p < 0.05$; **, $p < 0.01$ experimental value versus untreated control group.

fluorosis, which can dramatic disfigure the enamel bioceramic by imposing compromised aesthetics.[12]

This study showed that apoptosis of LS8 was directly linked to fluoride concentration. By electron microscopy, we observed ultrastructural changes to apoptotic cells that included peripheral chromatin condensation and endoplasmic reticulum expansion. These results are consistent with previous studies in odontoblasts and chondrocytes.[23,36] In addition, apoptotic cells showed the characteristic subcellular morphological features that included bleb formation, nuclear fragmentation, mitochondria swelling and formation of apoptotic bodies.[27]

Following treated by NaF, the expression levels for p-ERK and p-JNK in LS8-ameloblast like cells decreased proportionally with increasing NaF treatment concentrations compared to the control group. The decreased expression of p-ERK and p-JNK induced by NaF, as well as increased LS8 cell apoptosis presented themselves in a time and concentration dependent manner. These findings infer that both the p-ERK and p-JNK pathways participate in NaF- induced apoptosis of LS8 cells. ERK activation has been shown to influence the proliferation of dental epithelial cells during their development.[33] Other investigators reported that down-regulated expression levels of matrix metalloproteinase 20 (MMP-20) by fluoride was related to suppression of the JNK/c-Jun phosphorylation axis of signals.[28] Huang and colleagues reported that bioactive peptide amphiphile nanofibres bearing the integrin-binding epitope activated focal adhesion kinase (FAK) to increase phosphorylation of both JNK and its downstream transcription factor c-Jun (c-Jun) that served to up regulate amelogenin gene expression for enamel regeneration.[37] Karube and colleagues [21] found that activation of MAPKs in MDPC-23, a mouse odontoblast-like cell line, was induced by NaF cell treatment. In the study by Karube and colleagues, the increased expression of p-JNK, p38 and p-ERK presented themselves only after treated with NaF, after which their levels increased further. However, in this study, we found that p-JNK, p38 and p-ERK expression levels were detected even in the control group without F treatment. Their basal expression suggests that p-JNK, p38 and p-ERK are involved in the process of development/maturation of the LS8 cells. These pathways appear to play important roles in normal homeostasis of the LS8 cells, as well as in NaF-induced apoptosis.

Caspase effectors are a family of 13 members belonging to cysteine proteases. The caspase family is the common pathway for the apoptosis event, and therefore, their expression levels are important surrogate markers for apoptosis. In healthy cells, caspases are maintained as inactive zymogens.[38] The caspase-3 protein is a key enzyme in apoptosis and is known as the downstream 'effector' caspase. In contrast, caspases-8, -9 are classified as upstream 'initiator' caspase, functioning as the initiators of a proteolytic cascade by activating the procaspases that serve to biologically amplify the death signal. It is also well known that caspase-3 is activated

by caspase-8 and/or caspase-9, which play crucial roles in apoptosis induction through the intrinsic and/or the extrinsic pathways, respectively,[39] suggesting that cleaved caspase-12 can trigger apoptosis by indirectly activating caspase-3. In most cases, caspase activation is indispensable for complete cell apoptosis. In this study, the protein expression of caspase-3, -8, -9, and -12 decreased significantly with NaF-induced LS8 cell apoptosis and there was diminished expression of p-ERK and p-JNK. To further resolve the mechanism(s) involved for NaF-induced ameloblast-like cell apoptosis, the effects of inhibitors and agonists of the MAPK pathway were explored. The resulting data showed that inhibiting either the p-ERK or the p-JNK pathway decreased expression of caspase-3, -8, -9 and -12 proteins, although the degree of reduction was less than that was observed when NaF served as the trigger. The reason for this observation might be due to NaF collateral pathway activation, in which multiple pathways are triggered while largely only the one pathway was inhibited with specific inhibitors for p-ERK or p-JNK. In contrast, when the LS8 cell are treated with the agonist curcumin for p-ERK or the agonist anisomycin for p-JNK, no significant change in the expression levels of caspase-3, -8, -9 and -12 were observed. Comparing agonist treated to NaF treated cells, we observed less effects with the agonists compared to those observed with LS8 cells treated by NaF. These findings suggested that MAPK, and mainly the p-ERK and p-JNK paths, participated in the regulation of caspase -3, -8, -9 and -12 in the process of NaF-induced apoptosis of LS8 cells.

This may be the heart of the molecular mechanism for excessive fluoride-induced ameloblast apoptosis. As most investigators postulate that dental fluorosis is rooted in enamel hypomineralization caused by ameloblast apoptosis, the findings in this study may reveal the biological transduction pathway of F-induced apoptosis of ameloblast. It may be supposed that when ameloblast was explored to fluoride, the variation of expression level of p-ERK and p-JNK transferred the signal to caspase, which activate the proteolytic cascade of caspases, apoptosis of ameloblast happed. In addition, the finding of Huang and colleagues for increased FAK driving increased phosphorylation of both JNK and its downstream transcription factor c-Jun (c-Jun) that served to upregulate amelogenin gene expression [37] suggest that fluoride concentrations used in this study may lead to a loss of amelogenin protein expression during the formation of the enamel bioceramic matrix product. Lacruz and colleagues have shown enamel matrix formation and mineral deposition follow a circadian 24 h rhythm, with matrix production increased in one 12 h cycle and mineral deposition enhanced in the next 12 h cycle.[40] Amelogenin is the most abundant protein of the developing enamel and the loss of linkage between matrix production and mineral deposition brought about by the loss of enamel matrix formation may also contribute to the pathosis of dental fluorosis.

In addition, this study showed that different concentrations of NaF treatment increase p-p38 protein levels in apoptotic LS8 cells. Interestingly, pretreatment of LS8 cells by p38 inhibitor (SB203580) or by the independent mechanism of transducing p38 silencing RNA revealed NaF-induced alteration to caspases.[34] These results showed that suppression expression of p38 did not affect on NaF-induced expression level of caspase-3, -8, -9 and -12, which in turn suggested that p38 might not take a dominant role in NaF-induced apoptosis of LS8 cells. However, this interpretation does not agreed with the point that p38 and possibly the JNK is the pathway of fluoride induced apoptosis, which was the conclusion reached when epithelial lung cells were used to study fluorides.[16]

Among MAPK kinases, JNK and p38 pathways are frequently associated with induction of apoptosis, whereas the ERK pathways are thought to deliver survival signals that protect cells from apoptosis.[41] The p38 MAPK pathway is an important regulator of many cellular responses. It is well established that p38 MAPK signalling negatively regulates epithelial cell transformation, but enhanced p38 MAPK activity has been correlated with poor clinical prognosis in some neoplastic types. In this study, we found that ERK and JNK pathways take part in apoptosis. Although an increased expression of p38 was observed, no effect of p38 on caspases was identified. For these many reasons and unresolved implications, more studies of fluoride are needed.

Conclusions

During NaF-induced apoptosis of ameloblast like cell, p-ERK and p-JNK were closely associated with induction of apoptosis by regulating the expression level and the degree of activities of caspases, which may be the possible pathology reason of dental fluorosis; whereas the function of p38 pathway needs more experimental studies.

Acknowledgements

We thank Professor Yan Jin, of the Institute of Tissue Engineering and Regenerative Medicine, School of Stomatology, the Fourth Military Medical University for technical assistance.

Disclosure statement

The authors report no conflicts of interest. The authors alone are responsible for the content and writing of this article.

Funding

The National Natural Science Foundation of China [No. 30972558].

Notes on contributors

Lin Zhao, Associate Professor of Oral Pathology, PhD candidate interested in tooth development. Now, focus on the the mechanism and related effectors of tooth, especially, the enamel development.

Juedan Li, MD, A junior preventive dental specialist, interested in people's oral health, the molecular mechanism of dental fluorosis. Research area focus on the molecular mechanism of FoxO1 in dental fluorosis.

Jiali Su, MD, Dentist in department of Endodontics, interested in caries prevention and tooth development.

Malcolm L. Snead, PhD, Professor of the Biomedical Sciences, interested in biomineralization and biomaterials, tooth enamel.

Jianping Ruan, PhD, Professor of the Preventive Dentistry, interested in fluoride and dental health, caries prevention and tooth development.

Now, focus on the molecule and biological basis of dental fluorosis, the mechanism and related effectors of tooth, especially, the enamel development.

References

[1] Centers for Disease Control and Prevention. Achievements in public health, 1900–1999: fluoridation of drinking water to prevent dental caries. JAMA. 2000;283:1283–1286.

[2] Petersen PE, Lennon MA. Effective use of fluorides for the prevention of dental caries in the 21st century: the WHO approach. Community Dent Oral Epidemiol. 2004;32:319–321.

[3] Centers for Disease Control and Prevention. Ten great public health achievements–United States, 1900–1999. Morb Mortal Wkly Rep. 1999;48:241–243.

[4] Barbier O, Arreola-Mendoza L, Del Razo LM. Molecular mechanisms of fluoride toxicity. Chem Biol Interact. 2010;188:319–333.

[5] Ullah R, Zafar MS. Oral and dental delivery of fluoride: a review. Fluoride. 2015;48:195–204.

[6] Paine ML, Slots J, Rich SK. Fluoride use in periodontal therapy: a review of the literature. J Am Dent Assoc. 1998;129:69–77.

[7] Zafar MS, Ahmedb N. Therapeutic roles of fluoride released from restorative dental materials. Fluoride. 2015;48:184–194.

[8] Denbesten PK. Biological mechanisms of dental fluorosis relevant to the use of fluoride supplements. Community Dent Oral Epidemiol. 1999;27:41–47.

[9] Eby JD. A history of dentistry in Colorado, 1859–1959. Am J Orthod Dentofacial Orthop. 1961;47:310–312.

[10] Opydo-Szymaczek J, Gerreth K. Developmental enamel defects of the permanent first molars and incisors and their association with dental caries in the region of Wielkopolska, Western Poland. Oral Health Prev Dent. 2015;13:461–469.

[11] Aoba T, Fejerskov O. Dental fluorosis: chemistry and biology. Crit Rev Oral Biol Med. 2002;13:155–170.

[12] Denbesten PK, Li W. Chronic fluoride toxicity: dental fluorosis. Monogr Oral Sci. 2011;22:81–96.

[13] Elliott J, Scarpello JH, Morgan NG. Differential effects of genistein on apoptosis induced by fluoride and pertussis toxin in human and rat pancreatic islets and RINm5F cells. J Endocrinol. 2002;172:137–143.

[14] Goh EH, Neff AW. Effects of fluoride on *Xenopus* embryo development. Food Chem Toxicol. 2003;41:1501–1508.

[15] Otsuki S, Morshed SR, Chowdhury SA, et al. Possible Link between glycolysis and apoptosis induced by sodium fluoride. J Dent Res. 2005;84:919–923.

[16] Thrane EV, Refsnes M, Thoresen GH, et al. Fluoride-induced apoptosis in epithelial lung cells involves activation of MAP kinases p38 and possibly JNK. Toxicol Sci. 2001;61:83–91.

[17] Murao H, Sakagami N, Iguchi T, et al. Sodium fluoride increases intracellular calcium in rat renal epithelial cell line NRK-52E. Biol Pharm Bull. 2000;23:581–584.

[18] Yan X, Feng C, Chen Q, et al. Effects of sodium fluoride treatment in vitro on cell proliferation, apoptosis and caspase-3 and caspase-9 mRNA expression by neonatal rat osteoblasts. Arch Toxicol. 2009;83:451–458.

[19] Wang Z, Yang X, Yang S, et al. Sodium fluoride suppress proliferation and induce apoptosis through decreased insulin-like growth factor-I expression and oxidative stress in primary cultured mouse osteoblasts. Arch Toxicol. 2011;85:1407–1417.

[20] Ren G, Ferreri M, Wang Z, et al. Sodium fluoride affects proliferation and apoptosis through insulin-like growth factor I receptor in primary cultured mouse osteoblasts. Bio Trace Elem Res. 2011;144:914–923.

[21] Karube H, Nishitai G, Inageda K, et al. NaF activates MAPKs and induces apoptosis in odontoblast-like cells. J Dent Res. 2009;88:461–465.

[22] Yang S, Wang Z, Farquharson C, et al. Sodium fluoride induces apoptosis and alters bcl-2 family protein expression in MC3T3-E1 osteoblastic cells. Biochem Biophys Res Commun. 2011;410:910–915.

[23] Li P, Xue Y, Zhang W, et al. Sodium fluoride induces apoptosis in odontoblasts via a JNK-dependent mechanism. Toxicology. 2013;308:138–145.

[24] Lee JH, Jung JY, Jeong YJ, et al. Involvement of both mitochondrial- and death receptor-dependent apoptotic pathways regulated by Bcl-2 family in sodium fluoride-induced apoptosis of the human gingival fibroblasts. Toxicology. 2008;243:340–347.

[25] Bartlett JD, Dwyer SE, Beniash E, et al. Fluorosis: a new model and new insights. J Dent Res. 2005;84:832–836.

[26] Kubota K, Lee DH, Tsuchiya M, et al. Fluoride induces endoplasmic reticulum stress in ameloblasts responsible for dental enamel formation. J Biol Chem. 2005;280:23194–23202.

[27] Yang T, Zhang Y, Li Y, et al. High amounts of fluoride induce apoptosis/cell death in matured ameloblast-like LS8 cells by downregulating Bcl-2. Arch Oral Biol. 2013;58:1165–1173.

[28] Yan Q, Zhang Y, Li W, et al. Micromolar fluoride alters ameloblast lineage cells *in vitro*. J Dent Res. 2007;86:336–340.

[29] Simon HU, Haj-Yehia A, Levi-Schaffer F. Role of reactive oxygen species (ROS) in apoptosis induction. Apoptosis. 2000;5:415–418.

[30] Bogatcheva NV, Wang P, Birukova AA, et al. Mechanism of fluoride-induced MAP kinase activation in pulmonary artery endothelial cells. Am J Physiol Lung Cell Mol Physiol. 2006;290:L1139–L1145.

[31] Zhu Y, Wang Y, Zhao B, et al. Differential phosphorylation of GluN1-MAPKs in rat brain reward circuits following long-term alcohol exposure. PLoS One. 2013;8:e54930.

[32] Pfaffl MW. A new mathematical model for relative quantification in real-time RT-PCR. Nucleic Acids Res. 2001;29:e45.

[33] Cho KW, Cai J, Kim HY, et al. ERK activation is involved in tooth development via FGF10 signaling. J Exp Zool B Mol Dev Evol. 2009;312:901–911.

[34] Xu X, Han J, Ito Y, et al. Ectodermal Smad4 and p38 MAPK are functionally redundant in mediating TGF-beta/BMP signaling during tooth and palate development. Dev Cell. 2008;15:322–329.

[35] Lee MJ, Cai J, Kwak SW, et al. MAPK mediates Hsp25 signaling in incisor development. Histochem Cell Biol. 2009;131:593–603.

[36] Meng H, Zhang T, Liu W, et al. Sodium fluoride induces apoptosis through the downregulation of hypoxia-inducible factor-1alpha in primary cultured rat chondrocytes. Int J Mol Med. 2014;33:351–358.

[37] Huang Z, Newcomb CJ, Zhou Y, et al. The role of bioactive nanofibers in enamel regeneration mediated through integrin signals acting upon C/EBPalpha and c-Jun. Biomaterials. 2013;34:3303–3314.

[38] Mnich K, Carleton LA, Kavanagh ET, et al. Nerve growth factor-mediated inhibition of apoptosis post-caspase activation is due to removal of active caspase-3 in a lysosome-dependent manner. Cell Death Dis. 2014;5:e1202.

[39] Suliman A, Lam A, Datta R, et al. Intracellular mechanisms of TRAIL: apoptosis through mitochondrial-dependent and -independent pathways. Oncogene. 2001;20:2122–2133.

[40] Lacruz RS, Hacia JG, Bromage TG, et al. The circadian clock modulates enamel development. J Biol Rhythms. 2012;27:237–245.

[41] Wada T, Penninger JM. Mitogen-activated protein kinases in apoptosis regulation. Oncogene. 2004;23:2838–2849.